

# Localization Algorithm Based on a Spring Particle Model (LASPM) for Large-Scale Unmanned Aerial Vehicle Swarm (UAVs)

Sanfeng Chen, Shenzhen Institute of Information Technology, China\*

Guangming Lin, Dongguan City University, China

Tao Hu, Shenzhen Institute of Information Technology, China

Hui Wang, Shenzhen Institute of Information Technology, China

Zhouyi Lai, Shenzhen Institute of Information Technology, China

## ABSTRACT

A new localization algorithm based on large scale unmanned aerial vehicle swarm (UAVs) is proposed in the paper. The localization algorithm is based on a spring particle model (LASPM). It simulates the dynamic process of physical spring particle system. The UAVs form a special mobile wireless sensor network. Each UAV works as a highly-dynamic mobile sensor node. Only a few mobile sensor nodes are equipped with GPS localization devices, which are anchor nodes, and the other nodes are blind nodes. The mobile sensor nodes are set as particles with masses and connected with neighbor nodes by virtual springs. The virtual springs will force the particles to move to the original positions. The blind nodes' position can be inferred with the LASPM algorithm. The computational and communication complexity doesn't increase with the network scale size. The proposed algorithm can not only reduce the computational complexity, but also maintain the localization accuracy. The simulation results show the algorithm is effective.

## KEYWORDS

Computation Complexity, Localization Algorithm, Mobile Adhoc Network, Spring Particle Model, Unmanned Aerial Vehicle Swarm

## INTRODUCTION

The development of unmanned aerial vehicle (UAV) swarm poses a great challenge to the localization system of the UAVs (Chen et al., 2021). To swarming UAVs, their positions are essential for a variety of collaborative operations, including navigation(Chen et al., 2022), motion control(Wu et al.,2021), and mission completion (Gupta et al., 2016; Villas et al., 2013). There are a number of localization schemes(Moon et al., 2022; Mozaffari et al., 2019; Xiong et al., 2021), among which the global positioning system (GPS) is one of the most representative technologies

DOI: 10.4018/IJCI.333635

\*Corresponding Author

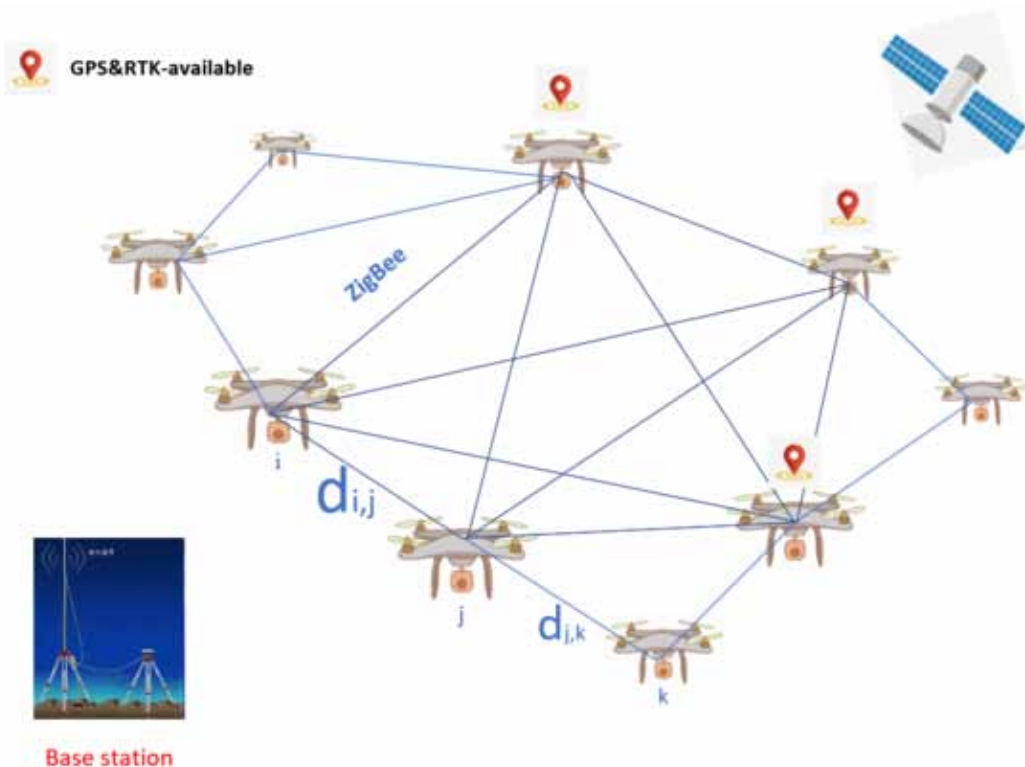
This article published as an Open Access article distributed under the terms of the Creative Commons Attribution License (<http://creativecommons.org/licenses/by/4.0/>) which permits unrestricted use, distribution, and production in any medium, provided the author of the original work and original publication source are properly credited.

(Youn et al., 2021; Goel et al., 2017). However, the location estimation performance of GPS has been found to be unreliable in some closed and isolated environments(Qi et al., 2020), such as urban canyons and indoor spaces (Zhou et al., 2019). The other localization and navigation methods, such as inertia navigation (Svacha et al., 2020), have large error accumulations that cannot be used in long-distance navigation (Gribben et al., 2014). Wireless sensor network technologies can be used for the UAVs' localization and navigation (Chen, et al., 2017). The wireless sensor nodes are deployed with the UAVs(Alzenad et al., 2017; Yang et al., 2017) . However, with the increase of operation area and scale of UAVs, a large number of sensor nodes need to be deployed(Alzenad et al., 2018;Kim et al., 2010), thereby constituting a large-scale wireless sensor network(Chen et al., 2018;Gao et al., 2021). A large-scale sensor network contains thousands of sensor nodes, and the complexity of the network becomes very sensitive to the sensors' scale(Yin et al., 2020). Examples include computational complexity, time complexity, and communication complexity. Now developing a low-complexity and high-energy efficient localization algorithm for large-scale sensor networks on UAVs is very urgent.

To solve these problems, we propose a UAV system with some movable Ultra Wideband (UWB) anchors. A base station controls several anchor UAVs. Each anchor UAV is equipped with a UWB anchor and real-time kinematic (RTK)-GPS capabilities. The blind nodes are equipped with CC2431 chips, which can be determined from the proposed LASPM algorithm by calculating the related forces with the neighbor anchor nodes. The diagram of a localization model for swarming UAVs is shown in Figure 1.

The LASPM localization algorithm is based on a spring model that is suitable for large-scale sensor networks. The complexity of each sensor node is  $O(1)$ , which does not increase proportionally

Figure 1. The diagram of localization model for swarming UAVs



with the scale of sensor networks. In this model, the sensor nodes are represented by particles with mass. The connection information between each pair of neighbor nodes is represented by a spring that connects this pair of nodes. The distance between this pair of neighbor nodes is represented by the original length of the spring. To localize the positions of blind nodes, we imagine that these blind particles are first drawn to random virtual positions by extra forces, and then these particles will go back to their stable positions virtually by the forces of springs.

In this paper we describe the LASPM localization algorithm, share the simulation results, and offer our conclusions.

## LOCALIZATION ALGORITHM BASED ON SPRING PARTICLE MODEL (LASPM)

The proposed localization algorithm is based on the following assumptions:

- The UAVs are deployed in a three-dimensional space.
- The UAVs form a dynamic network, which means that UAVs can add in or leave from the network at any time. In addition, the UAVs can fail at any moment.
- There are at least three anchor UAVs that know their accurate positions in the network. The other UAVs are blind nodes that do not know their positions. The anchor UAVs measure their positions with UWB and real-time kinematic (RTK)-GPS.
- The UAVs are able to communicate with UAVs that are in a radio range of  $R$ . UAVs in this range are named neighbor UAVs. The neighbor UAVs are in the same layer or the neighbor layer, which can't stride over another layer. Each UAV in the network owns a unique ID. The distances between the neighbor UAVs can be calculated with methods such as RSSI, TOA, and TDOA.
- The maximum velocity of UAV is 60 km per hr.
- The maximum size of UAVs is 200.
- The anchor UAVs and their related neighbor UAVs are in the same plane.
- Each UAV is simplified as a particle.

### Description of Localization Process

The localization process of UAVs is shown in Figure 2. The circles in the diagram represent the nodes of the sensor network. The nodes between the dashed lines can communicate directly (that is, they are in a radio range of  $R$ ). The localization algorithm works as a function. The input set includes the coordinates of anchor nodes  $Anchor(x, y, z)$  and relationship of neighbor nodes  $R_{Neighbor(i,j,k)}$ ; the output set includes the coordinates of blind nodes  $Node(x, y, z)$ , as shown in equation (1).

$$\frac{Set\{R_{Neighbor(i,j,k)}, Anchor(x, y, z)\}}{Localization\ Algorithm} \rightarrow Set\{Node(x, y, z)\} \quad (1)$$

The coordinate of anchor nodes is given as  $Anchor(x, y, z)$ . The coordinate of blind nodes can be resolved with the constraint condition based on the proposed spring and particle model.

### Model of Localization System

A spring particle system  $N = (P, S)$  is proposed to model a wireless sensor network system, where  $P$  is a particle set, and  $S$  is a spring set, as shown in Figure 3.

Each particle  $p_i \in P$  is associated with the sensor node  $i$  in the network, and each spring  $s_{ij} \in S$  is associated with the sensor node pair  $i, j$ . The distance between sensor node pair  $d_{ij}$  can be measured or calculated. There are four attributes of each particle:  $m$ ,  $r$ ,  $v$ , and  $a$ . The  $m$  attribute

Figure 2 The diagram of localization process of mobile WSN nodes

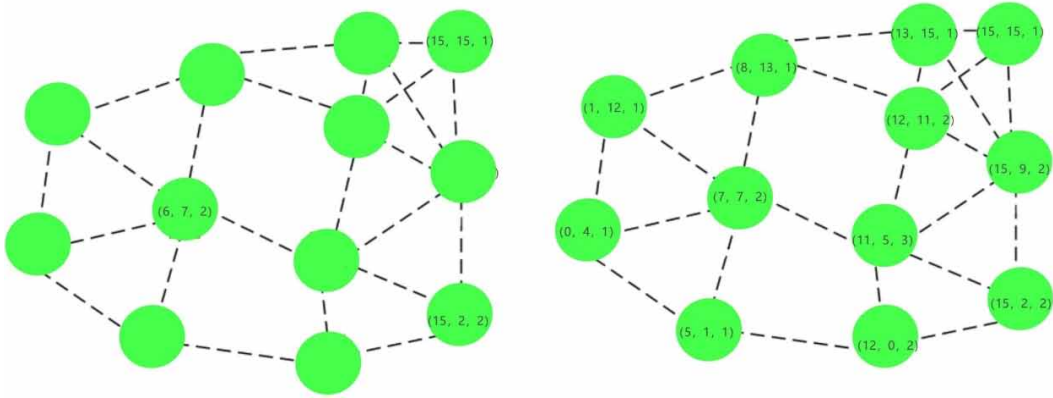
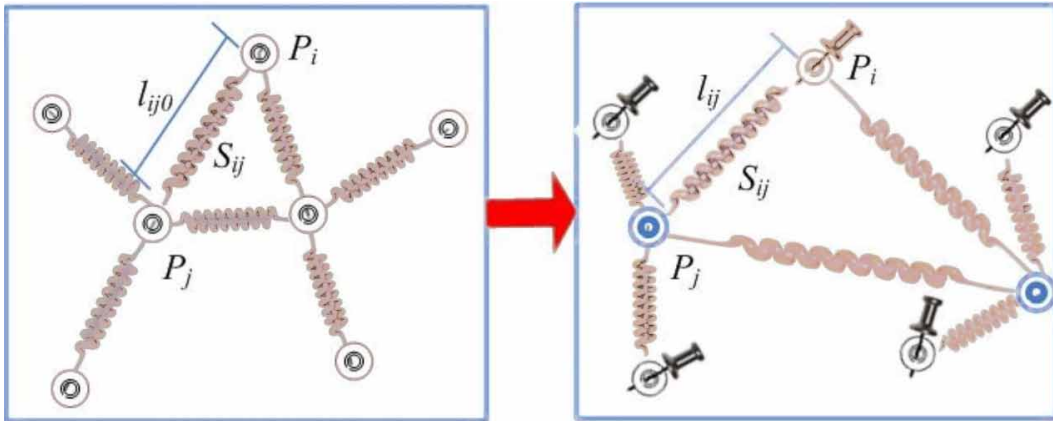


Figure 3 The spring particle model for wireless sensor networks



denotes the mass,  $r$  denotes the position,  $v$  denotes the velocity, and  $a$  denotes the acceleration. Each spring has two attributes:  $k$  and  $l_0$ . The  $k$  attribute denotes the constant coefficient of the spring, and  $l_0$  denotes the original length of the spring. The relationship between the node and the neighbor nodes is as follows:

- There is virtual spring force between any two neighbor nodes.
- The joint force of a particle is the vector sum of the virtual spring force.
- The sensor nodes are affected by the damping forces of the spring system. The damping forces are proportional to the velocity.
- The virtual mass of the sensor node is  $m$ , and the acceleration, velocity, and displacement can be calculated with Newton's second law of motion.

### Static and Dynamic Equations

To each spring  $s_{ij}$ , the joint force of the spring can be calculated using the formula shown in equation (2):

$$F_{i,j} = -k_{ij}(l_{ij} - l_{ij0}) \quad (2)$$

To each particle  $p_i$ , the sum force is as shown in equation (3):

$$\vec{F}_i = f(\vec{F}_{i,j}, \vec{v}_i) \quad (3)$$

Set  $\vec{F}_i$  as shown in equation (4):

$$\vec{F}_i = \sum_{s_{ijk} \in S} \vec{F}_{i,j} - \eta \vec{v}_i \quad (4)$$

In equation (4),  $\eta$  is the damping coefficient.

The acceleration of the particle  $i$  is shown in equation (5):

$$\vec{a}_i = \frac{\vec{F}_i}{m_i} \quad (5)$$

The discrete state equations for velocity and position are shown in equations (6) and (7):

$$\vec{v}_i(t + \Delta T) = \vec{v}_i(t) + \vec{a}_i(t) \cdot \Delta T \quad (6)$$

$$\vec{r}_i(t + \Delta T) = \vec{r}_i(t) + \vec{v}_i(t) \cdot \Delta T \quad (7)$$

To further explain the above equations, a simplified force model diagram of the spring-particle is shown in Figure 4. The virtual spring forces between node A and nodes B, C, and D are  $F(BA)$ ,  $F(CA)$ , and  $F(DA)$ ; these three forces can be either virtual attracting forces or virtual repelling forces. The virtual positions of nodes A and C are  $\vec{P}_a$  and  $\vec{P}_c$ . The original distance between node A and C is  $D$ , the spring coefficient between blind nodes is  $K$ , and the spring coefficient between blind node and anchor node is  $K_{anchor} \cdot K$ . The damping coefficient of nodes is  $\eta$ , the virtual mass is  $m$ , and the displacement vector is  $\vec{x}$ . The interaction force between blind nodes A and C is shown in equation (8):

$$\vec{F}(c, a) = K(\Delta D) (\vec{P}_c - \vec{P}_a) \quad (8)$$

If node C is an anchor node, then we use the formula in equation (9):

$$\vec{F}(c, a) = K_{anchor} \bullet K(\Delta D) (\vec{P}_c - \vec{P}_a) \quad (9)$$

In equation (9),  $\Delta D = \|\vec{P}_c - \vec{P}_a\| - D$ ,  $K_{anchor} \geq 1$ . The anchor nodes are more reliable and more powerful than other nodes.

The joint force of nodes A is calculated using the formula shown in equation (10):

$$\vec{F}_a = \sum_{\text{nodes } i} \vec{F}(i, a) \quad (10)$$

In equation (10), nodes  $i$  are the neighbor nodes of node A.

According to Newton's second law of motion, the acceleration of node A is as shown in equation (11):

$$\ddot{\vec{x}}_a(t) = \frac{F_a - \eta \dot{\vec{x}}_a}{m} \quad (11)$$

### The Localization Procedure

The localization procedure based on the spring particle model is shown in Figure 5. In process I, sensor nodes are deployed in a 3D space. The circles denote the nodes, and the solid lines denote the two nodes that are within the radio range. In process II, the wireless sensor network is represented by the spring particle system. The sensor nodes are represented by the particles. The distances between neighbor nodes are represented by the springs. As shown in process III, the anchor nodes have their actual absolute positions, so the anchor particles are fixed in their absolute positions. The blind particles are drawn to random positions. The springs between these blind particles are then stretched or compressed, making the total forces of the blind particles not equal to zero. Therefore, these blind particles will move according to equation (7). In process IV, these blind particles return to the stable positions where they are before. The positions can be obtained with equation (7). These positions are what need to be localized. The following items should be declared: each spring is virtual, which does not exist really. The position and velocity of each particle also changed virtually. Actually, the position of each blind node does not change.

### The Centralized LASPM Algorithm

In this paper, we assume that the centralized LASPM algorithm is executed on the sink nodes. The sink nodes are the most powerful UAVs, and they are equipped with GPS and RTK. The sink nodes are also equipped with more powerful computation ability and battery power than other nodes. In addition, the sink nodes are deployed in the medium layer by following these steps:

1. Each sensor node sends the distances between itself and its neighbors to the sink node. The anchor nodes also send their absolute positions to the sink node.

Figure 4. The interaction forces model of sensor nodes

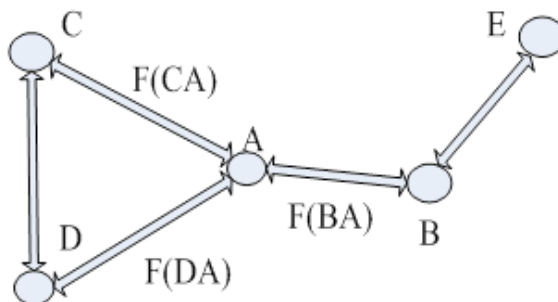
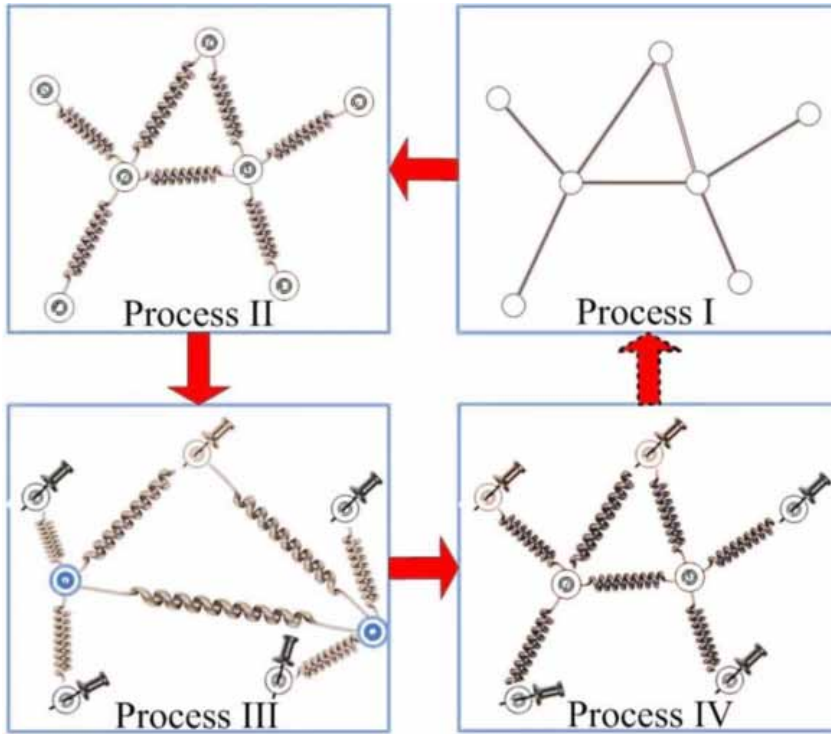


Figure 5. The process of the proposed localization algorithm based on spring particle model

Note: In Figure 5, I is wireless sensor network, II is spring model, III is setting blind particles in random positions, and IV is blind particles going back to their stable positions.



2. The sink node calculates the positions and velocities for all nodes using the formulas shown in equations 6 and 7.
3. Repeat step 2 until the total forces of all particles exerted by neighbor particles are smaller than a threshold  $T$  force, or  $L$  is larger than  $lstsep$ . Each sink node executes the localization algorithm in parallel model. Its computational complexity is  $O(1)$ ; therefore, the time complexity is also  $O(1)$ . The computational complexity, time complexity, and communication complexity are very appropriate for the large-scale sensor networks. In the centralized scheme, the total computational complexity is  $O(n)$ , which is also much smaller than that of other localization algorithms, such as MDS-MAP.

### Module and Theoretical Analysis for LASPM

The location of node  $i$  is calculated using the functions shown in equation (12):

$$\begin{cases} \sqrt{(x_i - x_j)^2 + (y_i - y_j)^2} = R_{i,j}^e \\ \sqrt{(x_i - x_k)^2 + (y_i - y_k)^2} = R_{i,k}^e \\ \sqrt{(x_i - x_l)^2 + (y_i - y_l)^2} = R_{i,l}^e \end{cases} \quad (12)$$

Node  $i$  is determined by the neighboring nodes' information, which makes the computational complexity and energy consumption much lower.

The Lyapunov stability functional  $V$  of the spring particle model is defined as shown in equation (13):

$$V = \frac{1}{4} \sum_{\{ij|s_{ij} \in S\}} k_{ij} (\vec{r}_i - \vec{r}_j - \vec{r}_{ij}) \cdot (\vec{r}_i - \vec{r}_j - \vec{r}_{ij}) + \frac{1}{2} \sum_{\{i|p_i \in P\}} m_i \dot{\vec{r}}_i \cdot \dot{\vec{r}}_i \quad (13)$$

In equation (13),  $\vec{r}_{ij}$  is the initial length vector of vector spring  $ij$  shown in equation (14):

$$\vec{r}_{ij} = r_{ij0} \frac{\vec{r}_i - \vec{r}_j}{\|\vec{r}_i - \vec{r}_j\|} \quad (14)$$

$dV / dt$  is defined as shown in equation (15):

$$\frac{dV}{dt} = \frac{1}{2} \sum_{\{ij|s_{ij} \in S\}} k_{ij} (\vec{r}_i - \vec{r}_j - \vec{r}_{ij}) \cdot (\dot{\vec{r}}_i - \dot{\vec{r}}_j) + \sum_{\{i|p_i \in P\}} m_i \dot{\vec{r}}_i \cdot \ddot{\vec{r}}_i \quad (15)$$

The first item is shown in equation (16):

$$\sum_{\{ij|s_{ij} \in S\}} k_{ij} (\vec{r}_i - \vec{r}_j - \vec{r}_{ij}) \cdot (\dot{\vec{r}}_i - \dot{\vec{r}}_j) = 2 \sum_{\{ij|s_{ij} \in S\}} k_{ij} (\vec{r}_i - \vec{r}_j - \vec{r}_{ij}) \cdot \dot{\vec{r}}_i \quad (16)$$

The second item is shown in equation (17):

$$\sum_{\{i|p_i \in P\}} m_i \dot{\vec{r}}_i \cdot \ddot{\vec{r}}_i = - \sum_{\{ij|s_{ij} \in S\}} k_{ij} (\vec{r}_i - \vec{r}_j - \vec{r}_{ij}) \cdot \dot{\vec{r}}_i - \sum_{\{i|p_i \in P\}} c_i \dot{\vec{r}}_i \cdot \dot{\vec{r}}_i \quad (17)$$

Therefore, 
$$\frac{dV}{dt} = - \sum_{\{i|p_i \in P\}} c_i \dot{\vec{r}}_i \cdot \dot{\vec{r}}_i$$

$dV / dt \leq 0$ , only when the total force and velocity for each particle are equal to zero,  $dV / dt \equiv 0$ . Therefore, with random initialization, the system is stable at the points where the total force of each particle is equal to zero. Because the LASPM algorithm simulates the physical process of the system, the LASPM algorithm is convergent.

The error functional  $Err$  is defined as shown in equation (18):

$$Err = \sum_{(i,j)} (\sqrt{(x_i - x_j)^2 + (y_i - y_j)^2} - r_{ij0})^2 \quad (18)$$

The minimum is as shown in equation (19):

$$\min(Err) = \min_{(i,j)} (\sqrt{(x_i - x_j)^2 + (y_i - y_j)^2} - r_{ij0})^2 \quad (19)$$

The *Err* is minimum when  $\frac{\partial Err}{\partial x_i} = 0, \frac{\partial Err}{\partial y_i} = 0$  ( $i = 1, \dots, n$ )

The total force of node  $i$  is as shown in equation (20):

$$F_i = \sum_{s_j \in S} F_{i,j} - \eta v_i = \sum_{\{j|s_j \in S\}} -k_{ij}(\vec{r}_i - \vec{r}_j - \vec{r}_{ij}) - \eta \vec{v}_i \quad (20)$$

The component of force in the direction of  $x$  is shown in equation (21):

$$F_{xi} = \sum_{\{j|s_j \in S\}} -k_{ij}(\vec{r}_i - \vec{r}_j - \vec{r}_{ij}) - \eta \vec{v}_i = \sum_{\{j|s_j \in S\}} -k_{ij} \left( \frac{\|\vec{r}_i - \vec{r}_j\| - r_{ij0}}{\|\vec{r}_i - \vec{r}_j\|} (x_i - x_j) \right) - \eta \vec{v}_{xi} \quad (21)$$

We found that when the spring is stable (that is, the particle is static), the total force equals zero, as shown in equation (22).

$$F_{xi} = -\frac{\partial Err}{\partial x_i} = 0 \quad (22)$$

Therefore, when  $k_{ij} = 2$  and the system is stable, we can conclude that the LASPM algorithm minimizes the error square sum when it is convergent at the point where each force exerted by the spring is near or equal to zero and the total force of each particle is equal to zero.

## SIMULATION RESULTS

To test the performance of the proposed algorithm, we conducted the following experiment. Two hundred nodes were deployed in the area of  $10 \times 10$  randomly, where 40 nodes are anchor nodes. The average error of measuring range of anchor nodes is 2%, and the average connectivity of the nodes is 20. The simulation results are shown in Figure 6. In Figure 6, the circles denote the 200 nodes' real locations, and the ends of lines denote the nodes' simulation results. The localization error of the blind nodes with the proposed algorithm is less than 2%.

We conducted another experiment in which 160 sensor nodes were deployed randomly in an area of  $10 \times 10$  forming a C-shaped network. The measured range error is 5%, and the average connectivity is 5.4, as shown in Figure 7.

We also got the following results shown in Figure 8. With the anchor nodes increasing, the position error is decreasing. The error is less than 10% when the anchor nodes range is more than 30%. The proposed algorithm is also sound in the C-shaped network.

## CONCLUSION

After theoretical study and computer simulation, the proposed LASPM algorithm has been proven efficient for large-scale UAV networks. We conclude that the localization algorithm based on spring particle model (LASPM) has low complexity in computation, communication, and time consumption because the calculation steps are almost constant while the node size increases. The simulation results of a sensor network with 40 to 200 nodes show that the calculation steps are  $150 \pm 50$  for different

Figure 6. The simulation results with regular network

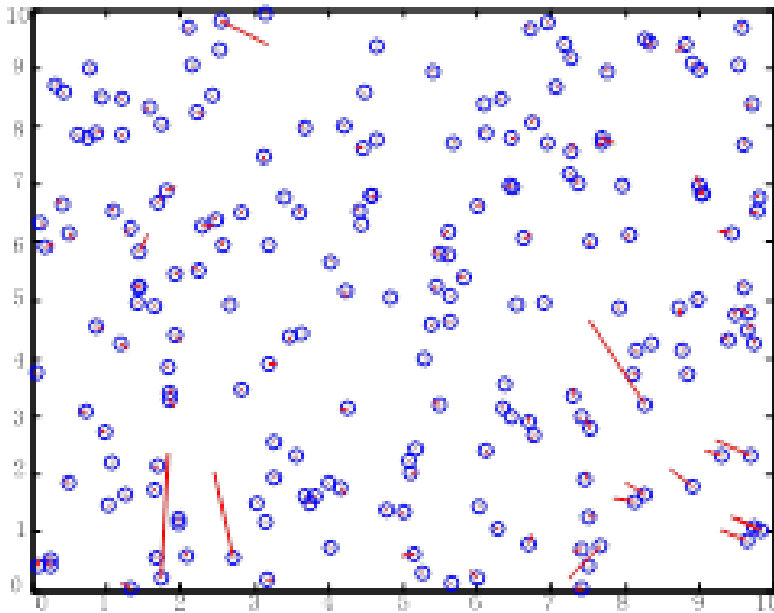
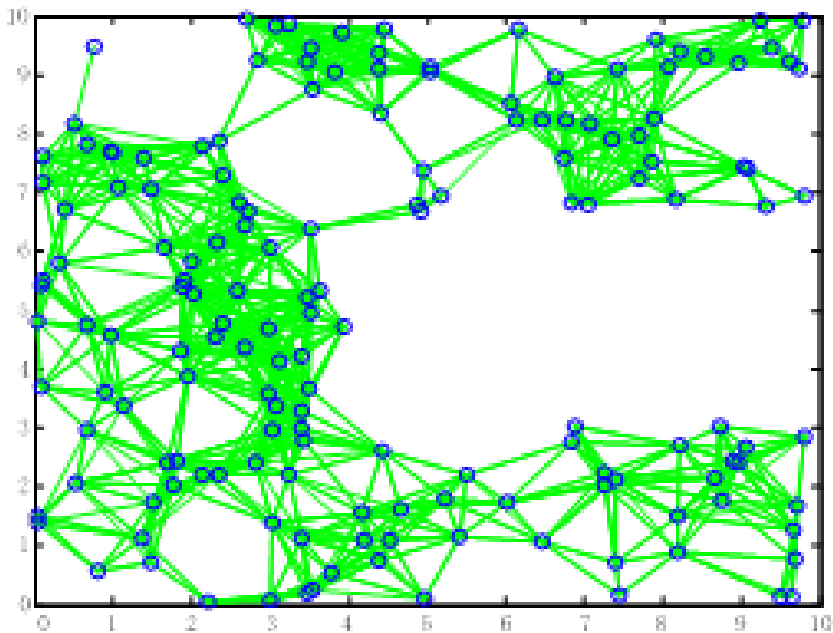
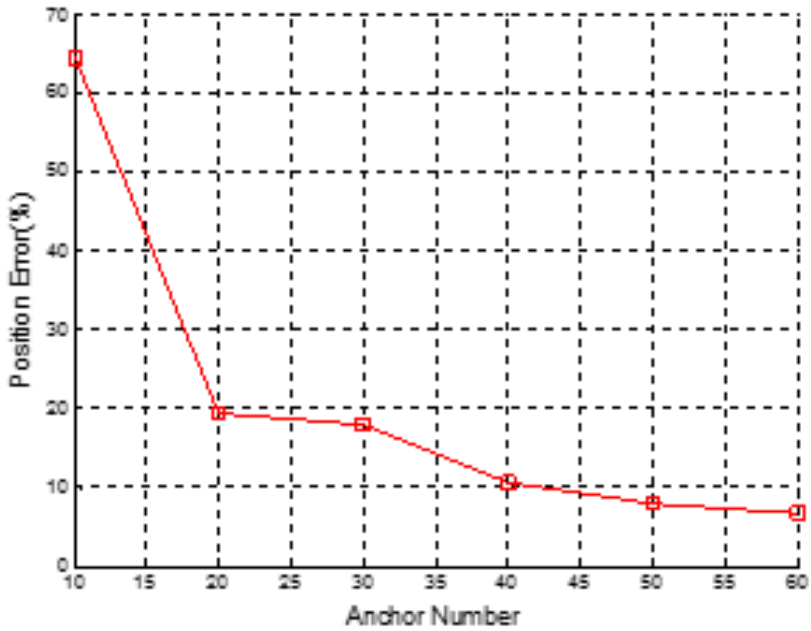


Figure 7. The simulation results with c-shaped network



node numbers. The localization accuracy is about 10% with the variety of sensor nodes. Future work includes optimizing the positions of anchor sensor nodes and increasing the network size for UAVs' localization and navigation.

Figure 8. The number of anchor nodes versus localization error



## ACKNOWLEDGMENT

We would like to acknowledge the support by the National Natural Science Foundation Youth Fund Project of China under Grant No. 62203310,

Guangdong Basic and Applied Basic Research Foundation under Grant No. 2022A1515011447, the Characteristic innovation projects of ordinary colleges and universities of Guangdong Province under Grant No. 2021KTSCX281, the Shenzhen Fundamental Research Fund under No. Grant 0220820010535001, the Science and Technology Project of SZIIT under Grant No.XQ2022B, and Zhouyi Lai Master Office of Robotics Integration.

## REFERENCES

- Alzenad, M., El-Keyi, A., & Yanikomeroglu, H. (2017). 3-D placement of an unmanned aerial vehicle base station (UAV-BS) for energy-efficient maximal coverage. *IEEE Wireless Communications Letters*, 6(4), 434–437. doi:10.1109/LWC.2017.2700840
- Alzenad, M., El-Keyi, A., & Yanikomeroglu, H. (2018). 3-D placement of an unmanned aerial vehicle base station for maximum coverage of users with different QoS requirements. *IEEE Wireless Communications Letters*, 7(1), 38–41. doi:10.1109/LWC.2017.2752161
- Chen, M., Xiong, Z., & Wang, R. (2022). Cooperative Navigation for Low-Cost UAV Swarm Based on Sigma Point Belief Propagation. *Remote Sensing (Basel)*, 14(9), 1976. doi:10.3390/rs14091976
- Chen, R., Yang, B., & Zhang, W. (2021). Distributed and collaborative localization for swarming UAVs. *IEEE Internet of Things Journal*, 8(6), 5062–5074. doi:10.1109/JIOT.2020.3037192
- Chen, S., Hu, T., & Lin, G. (2017). Derivative localization algorithm based on a spring particle model (LASPM) for large-scale wire sensor networks. *Chuanggan Jishu Xuebao*, 30(9), 1–7. doi:10.3969/j.issn.1004-1699.2017.09.018
- Chen, Y., Feng, W., & Zheng, G. (2018). Optimum placement of UAV as relays. *IEEE Communications Letters*, 22(2), 248–251. doi:10.1109/LCOMM.2017.2776215
- Gao, N., Zeng, Y., Wang, J., Wu, D., Zhang, C., Song, Q., Qian, J., & Jin, S. (2021). Energy model for UAV communications: Experimental validation and model generalization. *China Communications*, 18(7), 253–264. doi:10.23919/JCC.2021.07.020
- Goel, S., Kealy, A., Gikas, V., Retscher, G., Toth, C., Brzezinska, D.-G., & Lohani, B. (2017). Cooperative Localization of Unmanned Aerial Vehicles Using GNSS, MEMS Inertial, and UWB Sensors. *Journal of Surveying Engineering*, 143(4), 1016–1029. doi:10.1061/(ASCE)SU.1943-5428.0000230
- Gribben, J., & Boukerche, A. (2014). Location error estimation in wireless ad hoc networks. *Ad Hoc Networks*, 13(2), 504–515. doi:10.1016/j.adhoc.2013.10.007
- Gupta, L., Jain, R., & Vaszkun, G. (2016). Survey of Important Issues in UAV Communication Network. *IEEE Communications Surveys and Tutorials*, 18(2), 1123–1152. doi:10.1109/COMST.2015.2495297
- Kim, E., Lee, S., Kim, C., & Kim, K. (2010). Mobile beacon-based 3D localization with multidimensional scaling in large sensor networks. *IEEE Communications Letters*, 14(7), 647–649. doi:10.1109/LCOMM.2010.07.100513
- Moon, S., & Youn, W. (2022). A novel movable UWB localization system using UAVs. *IEEE Access : Practical Innovations, Open Solutions*, 10, 41303–41312. doi:10.1109/ACCESS.2022.3164701
- Mozaffari, M., Saad, W., Bennis, M., & Debbah, M. (2019). A Tutorial on UAVs for Wireless Networks: Applications, Challenges, and Open Problems. *IEEE Communications Surveys and Tutorials*, 21(3), 2334–2360. doi:10.1109/COMST.2019.2902862
- Qi, Y., Zhong, Y., & Shi, Z. (2020). Cooperative 3-D relative localization for UAV swarm by fusing UWB with IMU and GPS. *Journal of Physics: Conference Series*, 1642(1), 12–28. doi:10.1088/1742-6596/1642/1/012028
- Svacha, J., Paulos, J., Loianno, G., & Kumar, V. (2020). IMU-based inertia estimation for a quadrotor using Newton-Euler dynamics. *IEEE Robotics and Automation Letters*, 5(3), 3861–3867. doi:10.1109/LRA.2020.2976308
- Villas, L. A., Guidoni, D. L., & Ueyama, J. (2013). 3D localization in wireless sensor networks using unmanned aerial vehicle. *Proceedings of the 2013 IEEE 12th International Symposium on Network Computing and Applications*, 135–142. doi:10.1109/NCA.2013.35
- Wu, Y., Guan, X., Yang, W., & Wu, Q. (2021). UAV Swarm Communication Under Malicious Jamming: Joint Trajectory and Clustering Design. *IEEE Wireless Communications Letters*, 10(10), 2264–2268. doi:10.1109/LWC.2021.3099128
- Xiong, J., Cheong, J. W., Xiong, Z., Dempster, A. G., Tian, S., & Wang, R. (2021). Integrity for Multi-Sensor Cooperative Positioning. *IEEE Transactions on Intelligent Transportation Systems*, 22(2), 792–807. doi:10.1109/TITS.2019.2956936

- Yang, X., Gao, Z., & Niu, Q. (2017). Unmanned aerial vehicle–assisted node localization for wireless sensor networks. *International Journal of Distributed Sensor Networks*, 13(12), 1–13. doi:10.1177/1550147717749818
- Yin, S., Zhao, Y., Li, L., & Yu, F. (2020). UAV-Assisted Cooperative Communications With Time-Sharing Information and Power Transfer. *IEEE Transactions on Vehicular Technology*, 69(2), 1554–1567. doi:10.1109/TVT.2019.2956167
- Youn, W., Ko, H., Choi, H., Choi, I., Baek, J.-H., & Myung, H. (2021). Collision free autonomous navigation of a small UAV using low-cost sensors in GPS-denied environments. *International Journal of Control, Automation, and Systems*, 19(2), 953–968. doi:10.1007/s12555-019-0797-7
- Zhou, M., Wang, Y., Liu, Y., & Tian, Z. (2019). An information-theoretic view of WLAN localization error bound in GPS-denied environment. *IEEE Transactions on Vehicular Technology*, 68(4), 4089–4093. doi:10.1109/TVT.2019.2896482

*Sanfeng C. received her undergraduate degree and post graduate degree in Robotics from Jiangxi University of Science and Technology. She received PhD in Robotics from University of Science and Technology of China. She is currently working as an Associate professor in Shenzhen Institute of Information Technology. Her area of interest includes robotics and wireless Sensor Networks.*